Nanoscale

View Online
Dynamic Article Links

Cite this: *Nanoscale*, 2011, **3**, 2118

www.rsc.org/nanoscale

MINIREVIEW

Liquid-phase exfoliation, functionalization and applications of graphene

Xu Cui, Chenzhen Zhang, Rui Hao and Yanglong Hou*

Received 3rd February 2011, Accepted 7th March 2011
DOI: 10.1039/c1nr10127g

Graphene has attracted intense interest due to its exceptional physical and chemical properties as well as its wide potential applications. The processability and stability of this two-dimensional material in a variety of solvents have been the prerequisites for its functionalization, which will generate more interesting properties for further applications. In this mini review, we present and discuss the current status of liquid-phase exfoliation of graphene from various types of graphite, followed by a topical summarization of recent progress in the functionalization and applications of graphene.

1. Introduction

Graphene is the most basic building block for all its allotropic materials.[1,2] It can be wrapped up into 0D fullerenes,[3] rolled into 1D carbon nanotubes (CNTs)[4] and stacked into 3D graphite as illustrated in Fig. 1a. Intrinsic graphene is a semi-metal or zero-band gap semiconductor. Long-range and delocalized π-conjugation in the graphene plane endows itself with exceptional electrical, mechanical and thermal properties: ultrahigh intrinsic carrier mobility (~200 000 $cm^2\ V^{-1}\ s^{-1}$),[5] high thermal conductivity (~5000 $W\ m^{-1}\ K^{-1}$)[6] and Young's modulus (~1.0 TPa).[7,8] Specifically, single-layer graphene (SLG) shows unique electronic structure: band overlaps at two inequivalent conical points K and K′ (called Dirac points) in the first Brillouin zone (Fig. 1b).[9] In addition, because it only consists of one monoatomic layer, its theoretical optical transmittance can reach as high as 97.7%,[10] which, along with its high electrical conductivity, may find interesting applications in next generation transparent electrodes, especially on flexible substrates.[11–13]

Similar to other new materials, the availability and processability of graphene have been the prerequisites for its further applications. Early attempts to synthesize monolayer graphite could be traced back to 1975, when Lang found evidence of monolayer graphite by thermal decomposition of carbon on single-crystal Pt substrate.[14] Nevertheless, due to failure to identify its potential applications, graphene still remained "hidden" from the public. In 2004, Novoselov *et al.* employed a micromechanical exfoliation technique to successfully isolated two-dimensional crystal graphene from three-dimensional graphite onto a 300 nm oxidized silicon wafer and identified its potential applications in electronics,[1] which gradually unveiled this mysterious material. Since then, research efforts have followed up on developing new processing routes for efficient synthesis of high-quality and large-scale SLG. Until now, there have been several widely used methods to produce "pristine" graphene: micromechanical exfoliation,[1,15] liquid-phase

Department of Advanced Materials and Nanotechnology, College of Engineering, Peking University, Beijing, 100871, China. E-mail: hou@pku.edu.cn; Fax: + 86(10) 62753115

Yanglong Hou

Yanglong Hou received his PhD in Materials Science from Harbin Institute of Technology (China) in 2000. After a short post-doctoral training at Peking University, he worked at the University of Tokyo from 2002–2005 as JSPS foreign special researcher and also at Brown University from 2005–2007 as postdoctoral researcher. He joined Peking University in 2007, and now is a Professor of Materials Science. His research interests include the design and chemical synthesis of functional nanoparticles and graphene, and their biomedical and energy related applications.

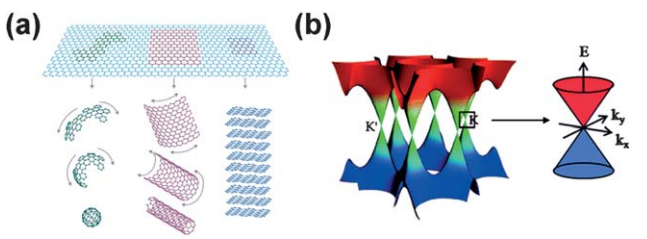

Fig. 1 (a) Graphene is the most basic building block for all its allotropic materials: fullerenes, CNTs and graphite. (b) Unique electronic band structure of SLG. Reproduced with permission from ref. 2 (a) and ref. 9 (b). Copyright: 2007 Nature Publishing Group (a) and 2009 Royal Society of Chemistry (b).

exfoliation,[16–18] epitaxial growth on SiC[19,20] and chemical vapor deposition (CVD) growth,[21,22] *etc.*

The large theoretical surface area (~2630 m^2 g^{-1}) of graphene,[23] which provides possibilities for its chemical functionalization, along with strong and flexible mechanical properties makes it promising in many applications. Modulation of its chemical and physical properties from the macroscopic to molecular scale has propelled a large share of the current research efforts.[24–29] Note that many reviews have summarized the up-to-date achievements of graphene and graphene-based materials.[9,30–36] From a different perspective, we review the research of the liquid-phase exfoliation of graphene, and then topically summarize the recent progress in its functionalization for various applications.

2. Liquid-phase exfoliation

Liquid-phase exfoliation is a widely used method to make colloidal dispersions of graphene in a variety of solvents. Its typical procedures involve exposure of graphite or graphite oxide powders to particular solvents, and then exposing these solutions to sonication. Based on the different starting graphite sources and exfoliation process, we generally summarize the current status of liquid-phase exfoliation into the following categories: liquid-phase exfoliations from graphite oxide, pristine graphite and expanded graphite (EG), and sonication-free liquid-phase exfoliation.

2.1 Liquid-phase exfoliation from graphite oxide

Graphene oxide (GO) can be easily exfoliated by sonication from graphite oxide which can be easily prepared by the Hummers method.[37] GO consists of an sp^2-bonded carbon structure occupied by a large number of covalently bonded hydroxyl or carboxyl groups which give GO a significant advantage as it can be dispersed in some organic solvents at concentrations of up to 1 mg mL^{-1} [25,38,39] and in water up to 7 mg mL^{-1}.[40] However, the oxidization process introduces significant defects in the as-made graphene, degrading its unique properties. Therefore, it is necessary to produce much less defective graphene and develop more effective reduction methods to obtain chemically reduced graphene (CRG). At early time, Stankovich *et al.* proposed to reduce a GO film in hydrazine at 100 °C for 24 h (Fig. 2).[38] In the following years, some other reducing agents were also developed such as hydroquinone,[41] sodium borohydride ($NaBH_4$).[42] Using a different chemical environment, Wang *et al.* developed an effective solvothermal reduction method which was carried out in *N*,*N*-dimethylformamide (DMF) at 180 °C by using hydrazine as the reducing agent.[43] The solvothermal process of GO with *N*-methyl-pyrrolidone (NMP) in the absence of hydrazine was also reported.[44] Recently, metal Fe was reported to reduce exfoliated GO.[45] Nevertheless, none of these reduction methods can recover the graphene structure completely and some oxygen-containing groups are still irremovable.

2.2 Liquid-phase exfoliation from pristine graphite

To minimize the oxide defects in graphene, Hernandez *et al.* developed a gentle method to produce high-quality graphene through dispersion and exfoliation of pristine graphite in certain

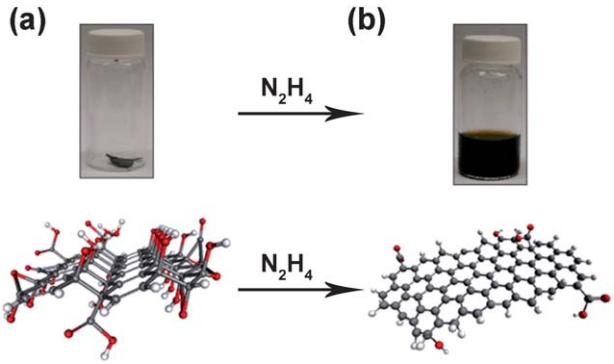

Fig. 2 (a) Graphite oxide paper in a glass vial. (b) The CRG dispersion after addition of hydrazine. Below each vial is a three-dimensional molecular model of graphite oxide (carbon in grey, oxygen in red and hydrogen in white) and CRG. Reproduced with permission from ref. 25. Copyright: 2009 Nature Publishing Group.

organic solvents which have been known to effectively disperse CNTs, such as NMP, DMF, γ-butyrolactone (GBL), 1,3-dimethyl-2-imidazolidinone.[18] After sonication of 30 min, followed by centrifugation (500 rpm, 90 min), the concentration of graphene dispersion can reach up to 0.01 mg mL^{-1}, and the monolayer yield was around 1 wt% in NMP, which could be potentially improved up to 7–12 wt% with further treatment. Although technically similar to the exfoliation of GO, this simple protocol differs essentially from it by the absence of the oxidation step. Among all of the test solvents, NMP provided the best thermodynamic stabilization due to the best matching surface energy with that of graphite (Fig. 3a). Raman spectra of individual flakes further identified defect-free monolayers or

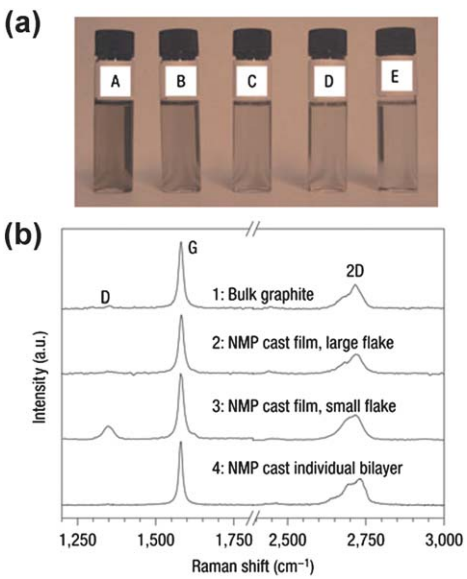

Fig. 3 (a) Dispersions of graphite flakes in NMP, at a range of concentrations from 6 μg mL^{-1} (A) to 4 μg mL^{-1} (E) after centrifugation. (b) Raman spectra of bulk graphite (1), a vacuum filtered film with the laser spot focused on a large (~5 μm) flake (2), a vacuum filtered film with the laser spot focused on a small (~1 μm) flake (3), a large (~10 μm) bilayer (4). Reproduced with permission from ref. 18. Copyright: 2008 Nature Publishing Group.

multilayers from absence of the D band and the shape of 2D band, confirming the high quality of the graphene (Fig. 3b).

It is demonstrated that the success of such exfoliation depends on the small net energetic cost of the whole process.[18] This energy balance can be expressed as the enthalpy of mixing per unit volume, which can be derived as:

$$\frac{\Delta H_{\text{mix}}}{V_{\text{mix}}} \approx \frac{2}{T_{\text{flake}}}(\delta_{\text{G}} - \delta_{\text{sol}})^2 \phi$$

where δ is the square root of the surface energy of graphite or solvents (the surface energy of graphite is defined as the energy per unit area minimum required to overcome the van der Waals forces when peeling two sheets apart), T_{flake} is the thickness of a graphene flake and ϕ is the volume fraction of graphene. The matching of graphene and solvent surface energies is one criterion for a successful exfoliation process: the closer the graphene and solvent surface energies are, the smaller the enthalpy of mixing is, and the higher degree of exfoliation will be.

A range of solvents with varying surface energies were tested to exfoliate graphite into dispersions as shown in Fig. 4. The concentration of resulting graphene (after centrifugation) showed a peak for surface energy close to 40 mJ m^{-2} which matched with the reported values for the surface energy of graphite.[46,47] This implies the possible surface energy criterion for graphene exfoliation. As the surface energy of water (72.75 mJ m^{-2}) is much higher than this criterion, surfactants are employed to tune the water surface energy to a proper level for aqueous processed exfoliation. Lotya *et al.* used water and sodium dodecyl benzene sulfonate to exfoliate graphite with the aid of sonication.[48] As a result, more than 40% of these graphene flakes were less than five layers, with 3% of flakes consisting of monolayers, and showed to be free of defects under atomic resolution transmission electron microscopy and Raman spectra. Due to the adsorbed surfactant and charged surface of graphene, the dispersed flakes were relatively stable against aggregation. However, the concentration was still very low within a range from 0.002 to 0.05 mg mL^{-1}, much lower than dispersion from NMP exfoliation. Recently, the concentration of water/sodium cholate exfoliated graphene dispersion was reported to reach up to 0.3 mg mL^{-1} after an ultralong sonication time.[16]

These essential properties of solvents also play a significant role in avoiding graphene aggregation. Recent theoretical work by means of molecular dynamics simulations and the kinetic theory of colloid aggregation has elucidated the stabilization mechanism of liquid-phase exfoliated graphene, and demonstrated their dispersion ability as follows: NMP ~ DMSO > DMF > GBL > H_2O, which is quite consistent with the reported experimental results.[49]

In addition to the organic and inorganic solvents discussed above, ionic liquids (ILs) are another promising candidate. IL is considered as a "green solvent" due to its unique properties such as negligible vapour pressure, low toxicity and high chemical stabilities. Most importantly, IL has a surface tension closely matched with that of graphite, which is the key prerequisite of solvents for direct exfoliation.[50] It was reported that stable and highly concentrated suspensions (0.95 mg mL^{-1}) of non-oxidized few-layer graphene (FLG) was obtained *via* tip sonication of natural graphite flakes in the IL such as 1-butyl-3-methylimidazolium bis(trifluoromethanesulfonyl)imide ([Bmim][Tf_2N]).[51]

2.3 Liquid-phase exfoliation from expanded graphite

High temperature or microwave treatments have been employed to expand graphite for better liquid-phase exfoliation.[52–54] Graphite intercalation compounds (GICs) are also widely used as starting materials for exfoliation.[55–57] Our group, using thermally EG as the starting material, showed that monolayer and bilayer graphene could be produced by a solvothermal-assisted exfoliation process in acetonitrile (ACN), with the production of monolayer and bilayer graphene nanosheets (GNS) around 10 wt% (Fig. 5).[52] Recently, it was reported that large-flake graphene up to 300 μm^2 can be exfoliated from graphite by oleylamine in solvothermal conditions, with a high concentration of 0.15 mg mL^{-1}.[58]

The insolubility of graphite is another key factor limiting the degree of liquid-phase exfoliation. To tackle this problem, chemical modification of graphite has been explored for facilitating their solubility and subsequent exfoliation. For example, Sun *et al.* used *in situ* diazonium reactions to bond 4-bromophenyl onto the surface of EG, and followed by mild sonication in DMF. These functionally-assisted exfoliated graphene had

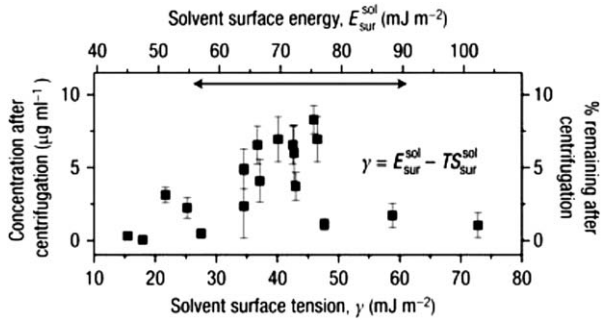

Fig. 4 Graphene concentration measured after centrifugation for a range of solvents plotted *versus* solvent surface tension. Shown on the right axis is the percentage of material remaining after centrifugation. The horizontal arrow shows the approximate range of the reported literature values for the surface energy of graphite. Reproduced with permission from ref. 18. Copyright: 2008 Nature Publishing Group.

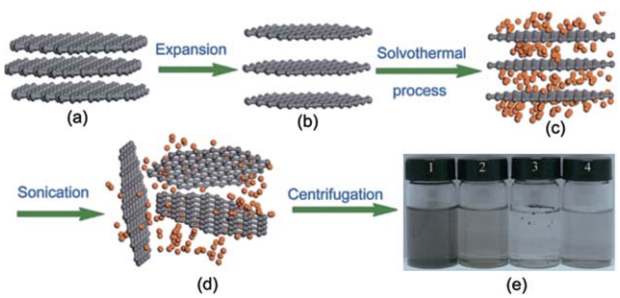

Fig. 5 Illustration of solvothermal exfoliation: (a) pristine graphite; (b) EG; (c) insertion of ACN molecules into the interlayers of EG; (d) exfoliated GNS dispersed in ACN; (e) samples under different conditions: solvothermal process (1) 600 rpm, 90 min; (2) 2000 rpm, 90 min; solvothermal-free process (3) 600 rpm, 90 min; (4) 2000 rpm, 90 min; Reproduced with permission from ref. 52. Copyright: 2008 Springer.

higher solubility than pristine graphene without any stabilizer additive of which more than 70% of these soluble flakes had less than five layers.[59] Recently, our group developed aqueous dispersed graphene solution using 7,7,8,8-tetracyanoquinodimethane (TCNQ)-anion as stabilizer and EG as starting material, which could also provide high-quality water soluble graphene for various applications.[60]

In 2008, Li *et al.* developed a liquid-phase method to exfoliate graphene nanoribbons (GNRs), with the assistance of poly(*m*-phenylenevinylene-*co*-2,5-dioctoxy-*p*-phenylenevinylene) (PmPV), directly from EG for potential molecular electronics (Fig. 6).[61] It involved exfoliating expandable graphite at 1000 °C and 30-min sonication of EG in the 1,2-dichloroethane (DCE) solution. The polymer PmPV, which noncovalently functionalized the graphene, played a role in π-interaction with conjugated plane and consequently stabilized nanoribbons in a homogeneous suspension. GNRs are materials with different properties from graphene sheets.[62–65] The all-semiconducting nature of sub-10 nm GNRs could solve the problem of the lack of bandgap in the pristine graphene. Electrical transport experiments on these exfoliated GNRs demonstrated, unlike single-walled CNTs, that all of the sub-10 nm GNRs were semiconductors with on–off ratios of about 10^7 at room temperature. After evaluation of all the GNR devices with varying widths from ~sub-10 to ~55 nm, the bandgap was fitted inversely proportional to their width.[65]

Although GNRs appear to be a promising candidate to replace CNT for future nanoelectronics, making GNRs using lithographic,[64,66] chemical,[67–69] and liquid-phase exfoliation[61] methods is still at the initial stages before scalable fabrication. Recently, well-designed GNRs were obtained from exfoliating multi-walled CNTs by Ar plasma[63] or solution-based oxidation process using $KMnO_4$,[62] which proposed a new concept for the production of GNRs. Besides, thick carbon nanoribbons could also be produced directly from graphite through an electrochemical process by anionic intercalation and oxidative cleavage.[70] With these merits of GNRs, the next major challenge is to find an efficient and reliable way to synthesize GNRs in solution.

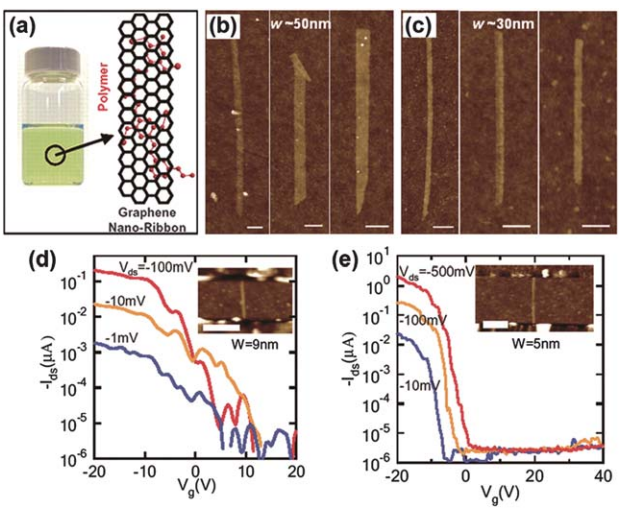

Fig. 6 (a) Photograph of a polymer PmPV/DCE with GNRs stably suspended in solution. (b, c) AFM images of selected GNRs with widths ~50 nm, ~30 nm. (d) Transfer characteristics for a $w \sim 9$ nm (two layers) and channel length $L \sim 130$ nm GNR with Pd contacts and Si backgate. (e) Transfer characteristics for a $w \sim 5$ nm (two layers) and channel length $L \sim 210$ nm GNR with Pd contacts. All scale bars: 100 nm. Reproduced with permission from ref. 61. Copyright: 2008 American Association for the Advancement of Science.

2.4 Sonication-free liquid-phase exfoliation

Supercritical CO_2 exfoliation. A supercritical CO_2 processing technique was reported for intercalating and exfoliating layered graphite to graphene. Specifically, FLG was produced by immersing powdered pure graphite in the atmosphere of supercritical CO_2 for 30 min and followed by rapidly depressurizing the supercritical fluid to expand and exfoliate graphite. The graphene sheets were collected by discharging the expanding CO_2 gas directly into a solution with sodium dodecyl sulfate to avoid restacking.[71]

Electrochemical exfoliation. The IL modified graphite can be exfoliated into graphene through one-step electrochemical approach by applying static potential bias between the two graphite rods.[70,72] The exfoliation mechanism is due to a complex interplay of anodic oxidation of water and anionic intercalation from IL.

Self-exfoliation in liquid phase. Graphene can also be self-exfoliated by induced strong repulsions between the interlayers. For example, GICs such as K(tetrahydrofuran)$_x$C$_{24}$ dissolved in NMP could spontaneously exfoliate into stable, air-sensitive solutions of graphene sheets without sonication due to strong negative charge repulsions (Fig. 7a).[73] Recently, Behabtu *et al.* demonstrated that graphite could be spontaneously exfoliated into SLG in chlorosulfonic acid, and dissolved at isotropic concentrations as high as 2 mg mL^{-1}, which was an order of magnitude higher than previously reported values (Fig. 7b).[74] Similarly, such exfoliation also resulted from the strong repulsions induced by acid protonated graphene interlayers. The

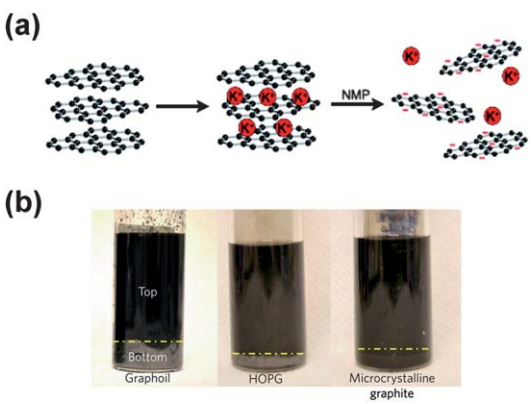

Fig. 7 (a) Negatively charged graphene layers from a GIC spontaneously dissolve in NMP. (b) Comparison of chlorosulfonic acid dispersion of graphite obtained from different sources as indicated below the vials. Reproduced with permission from ref. 73 (a) and ref. 74 (b). Copyright: 2008 American Chemical Society (a) and 2010 Nature Publishing Group (b).

resulting highly concentrated isotropic liquid phases are promising for scalable manufacture of nanocomposites, films and high-performance fibers.

3. Functionalization for applications

Modifying the surface of graphene (basal planes or edges) by bringing foreign atoms or molecules onto the surface through chemical bonding, van der Waals forces or π–π interactions can modulate the properties of graphene for various applications such as strengthening GO paper, field effect transistors (FETs), electrochemical sensors, chemical catalysts and energy storage and conversion devices.

3.1 Strengthening graphene oxide paper

Theoretical simulations and experimental studies of the mechanical properties of graphene, including Young's modulus and fracture strength, predict that graphene and graphene-based materials may possess superior mechanical properties,[7,8,75–77] which lays a solid foundation for its other applications. Individual defect-free graphene has a Young's modulus of 1.0 TPa and a fracture strength of 130 GPa.[7] In contrast, the CRG obtained by reducing GO with hydrogen plasma exhibited a lower elastic modulus of 0.25 TPa.[78] The mechanical properties of individual functionalized graphene are rarely reported. Another graphene-based novel material is GO paper which can be made by filtration or flow-directed assembly.[79] The average elastic modulus and the highest fracture strength were 32 GPa and 120 MPa, respectively. The mechanical properties of this GO paper could be improved by cross-linking the individual platelets using divalent ions (Mg^{2+} and Ca^{2+})[80] or poly(allylamine) hydrochloride.[81] In both cases, significant enhancement in mechanical stiffness and fracture strength of GO paper compared with the unmodified graphene could be attributed to an increase in the interlayer cross-linking by bonding between the GO sheets and functional counterparts.

3.2 Field effect transistors

Although graphene has shown great potential for next generation nanoelectronic devices in replacement of silicon, one of the biggest challenges for graphene is the lack of a bandgap in its electronic spectra. Another problem is that most of the as-made graphene FETs are p-type owing to unintentional doping by species absorbed from the ambient such as oxygen or water. Several methods have been developed to deal with these bandgap engineering issues. In addition to substrate[82] and confined-dimensions[61] induced bandgap, an alternative approach is to dope exotic atoms or chemical groups in the lattice or edges that can also open the bandgap.

In recent years, various studies of the electronic transport in nitrogen-doped (*N*-doped) graphene FETs, both theoretically and experimentally, have been presented.[24,26,83–85] Wei *et al.* reported the preparation of N-doped FLG by adding NH_3 during the CVD process at a temperature of 800 °C, exhibiting an n-type behaviour.[26] N-Type FETs obtained by nitrogen doping graphene materials *via* electrothermal reactions of GNRs[24] (Fig. 8a, b) or high temperature annealing of GO in NH_3 have been demonstrated.[84] Sinitskii *et al.* performed a kinetics study of diazonium

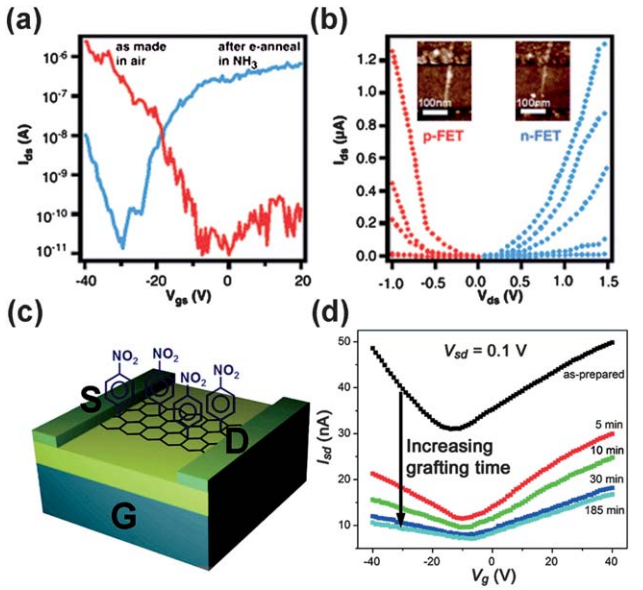

Fig. 8 (a) $I_{ds} - V_{gs}$ curves of the as-made GNR FET in vacuum (p-type, red) and after electron-annealing in NH_3 (n-type, blue). $V_{ds} = 1$ V for both curves. (b) $I_{ds} - V_{ds}$ curves of the same device. Red curves were taken on an as-made device: $V_{gs} = -40$ V, −37 V, −34 V, −31 V, and −28 V from top to bottom. Blue curves were taken on electron-annealed device: $V_{gs} = 40$ V, 35 V, 30 V, 25 V, and 20 V from top to bottom. (c) Schematic of the chemical functionalization of GNR devices with 4-nitrophenyl groups. (d) $I_{sd} - V_g$ curves for the same electronic device as a function of grafting time. Reproduced with permission from ref. 24 (a, b) and ref. 86 (c, d). Copyright: 2009 American Association for the Advancement of Science (a, b) and 2010 American Chemical Society (c, d).

salts functionalization of GNRs and showed that they could monitor the electrical properties of GNR FETs (Fig. 8c, d).[86]

3.3 Electrochemical sensors

Graphene is a promising electrode material due to its large surface area[23] which facilitates the electron transport along its surface. As exotic molecular disruption on the intrinsic graphene electronic structure can be easily detected, graphene-based sensors are expected to be highly sensitive for detecting individual molecules on and off its surface.[87–90]

For example, graphene sheets decorated with Pt and Pd nanoparticles (NPs) (Fig. 9a) displayed sensitive and fast response to glucose.[88] The presence of Pt and Pd NPs increased the electroactive area of the electrodes and substantially decreased the over-potential in the detection of hydrogen peroxide. Furthermore, the Pt/graphene glucose biosensor had a sensitivity of 61.5 ± 0.6 μA mM^{-1} cm^{-2} and gave a linear response of up to 20 mM, with a detection limit of 1 μM (Fig. 9b). In another example, cationic polyelectrolyte poly(diallyldimethyl ammonium chloride) functionalized graphene sheets with high loading Au NPs enhanced the performance for H_2O_2 sensing.[89] It is also worth noting that GO on the 3-aminopropyltriethoxysilane (APTES) modified electrodes could be directly reduced through an electrochemical process.[91] The reduced GO adsorbed on glassy carbon (GC) electrodes were modified with glucose oxidase by covalent bonding *via* a polymer

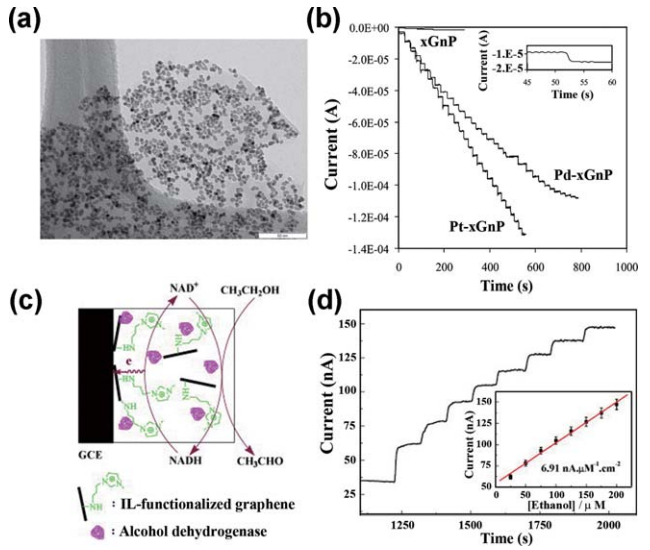

Fig. 9 (a) TEM image of Pt/graphene. (b) Amperometric responses for as-exfoliated graphene, Pt/graphene, and Pd/graphene glucose biosensors upon subsequent addition of 0.5 mM glucose solution (10 times) and then 1.0 mM glucose solution in 50 mM phosphate buffer solution (PBS) at 700 mV. (c) Schematic representation for the bioelectrocatalytic sensing of ethanol using IL-graphene/chitosan/ADH modified electrode. (d) Chronoamperometric response of IL-graphene/chitosan/ADH modified electrode in 5 mg mL^{-1} NAD^+ PBS (0.05 M, pH 7.4) on injecting the ethanol in 25 μM steps at working potential of 0.45 V. Reproduced with permission from ref. 88 (a, b) and ref. 90 (c, d). Copyright: 2008 American Chemical Society (a, b) and 2010 Elsevier (c, d).

generated by electrografting *N*-succinimidyl acrylate and the modified GO electrodes were also successfully used to detect glucose. Recently, an IL-functionalized graphene electrode was reported for low-potential NADH detection (440 mV decrease) and biosensing for ethanol.[90] The IL-graphene/chitosan/alcohol dehydrogenase (ADH) modified electrode biosensor showed rapid and highly sensitive amperometric response to ethanol with a low detection limit of 5 μM (Fig. 9 c, d).

3.4 Chemical catalysts

The large surface area of graphene can serve as a host material for metal NPs and its convenience in charge transfer provides a new way to develop advanced catalysts.[92] For example, chemically converted graphene (CCG) with 3,4,9,10-perylene tetracarboxylic acid (PTCA) and Au-ionic liquid (Au-IL) (CCG/PTCA/Au-IL) composites exhibited good electrocatalytic behavior toward oxygen reduction.[93] It was demonstrated that the modification of CCG with Au-IL could play an important role in increasing the electrocatalytic activity of CCG (Fig. 10a, b). Many studies implied that graphene should be a favourable candidate for the catalyst supports in methanol oxidation. It was reported that graphene-supported Pt or Pt/Ru NPs displayed excellent electrocatalytic activity for methanol oxidation.[94,95] Recently, $PtRu/PMo_{12}$/graphene catalysts were synthesized and exhibited higher electrocatalytic activity and better electrochemical stability for methanol oxidation compared with the PtRu/graphene catalysts.[96]

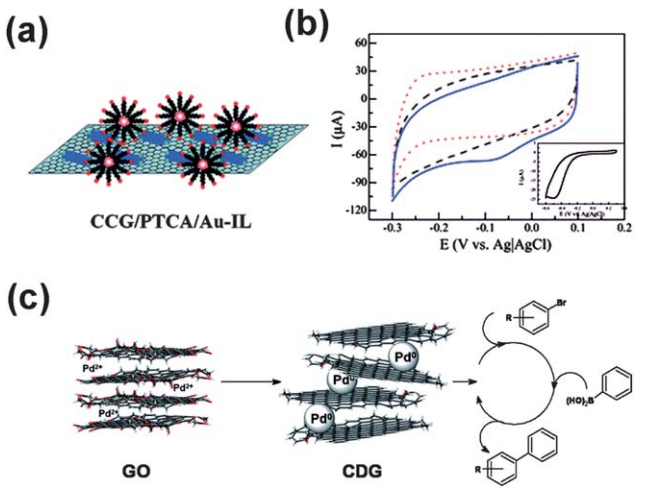

Fig. 10 (a) Illustration of CCG/PTCA/Au-IL composites. (b) Cyclic voltammograms (CVs) of CCG/PTCA/Au-IL-modified GC electrode in 0.5 M H_2SO_4 solution saturated with O_2 (solid) and N_2 (dotted); CCG/PTCA-modified GC electrode in 0.5 M H_2SO_4 solution saturated with O_2 (dashed). Inset: bare GC electrode in 0.5 M H_2SO_4 solution saturated with O_2. Scan rate: 0.05 V s^{-1}. (c) Illustration of Pd/graphene as highly active catalysts for Suzuki–Miyaura Coupling Reaction. Reproduced with permission from ref. 93 (a, b) and ref. 28 (c). Copyright: 2009 Royal Society of Chemistry (a, b) and 2009 American Chemical Society (c).

Selective electrochemical analysis could be achieved due to the selective catalysis of metal/graphene nanocomposites. Scheuermann *et al.* reported that the Pd/graphene composite catalysts were successfully applied to the Suzuki–Miyaura coupling reaction (Fig. 10c).[28] Recently, graphene modified with Au NPs was also used to act as efficient catalysts for the Suzuki reaction in water under aerobic condition.[97] Furthermore, the catalytic activity of Au NPs/graphene hybrids was influenced by the size of Au NPs.

Besides metal NPs, N-doped graphene prepared by nitrogen plasma treatment displayed excellent electrocatalytic activity for the reduction of hydrogen peroxide.[98] Noncovalent functionalization of CRG with methylene green exhibited a lower charge transfer resistance and better electrocatalytic activity toward the oxidation of NADH, compared with pristine CRG.[99]

3.5 Energy storage and conversion devices

The merits of graphene-based electrodes for applications in energy storage and conversion devices, such as rechargeable lithium ion batteries (RLBs), supercapacitors and solar cells have been widely reported recently.[29,100–105]

The key to increase the energy densities and cycling performance of RLBs is to optimize the anode materials. Many research attempts have been made to design new graphene-based electrode materials, especially metal oxide/graphene composites. The specific capacity of GNS was found to be 540 mAh g^{-1}, which was much larger than that of graphite. With addition of macromolecules of CNTs and C_{60}, it increased to 730 and 784 mAh g^{-1}, respectively.[100] Such increased storage capacity is due to the increase of interlayers distance between the graphene platelets intercalated by CNTs or C_{60} molecules. Following this work, Paek *et al.* further found that SnO_2/GNS electrodes

exhibited a reversible capacity of 810 mAh g^{-1} (Fig. 11a, b) with its drastically enhanced cycling performance compared with that of the bare SnO_2 NPs.[101] The dimensional confinement of SnO_2 NPs by the surrounding GNS limited the volume expansion upon lithium insertion, and the developed pores between SnO_2 and GNS could be used as buffered spaces during charge and discharge, resulting in the superior cyclic performances. Wang *et al.* developed an anionic surfactant mediated growth of self-assembled TiO_2/graphene hybrid nanostructures.[29] The nanostructured graphene hybrid materials showed enhanced Li-ion insertion and extraction kinetics in TiO_2, especially at high charge and discharge rates. Co_3O_4/graphene composites were reported to exhibit a large reversible capacity (935 mAh g^{-1} after 30 cycles), excellent cyclic performance, high Coulombic efficiency (above 98%) and good rate capability.[102] Recently, Fe_3O_4/GNS composite electrodes showed a high reversibility, and its reversible capacity even gradually increased to 1026 mAh g^{-1} after cycling (Fig. 11c, d).[103]

Supercapacitors, as a system between dielectric capacitor and battery, have attracted great interest recent years. Due to its different mechanism of storing electrical energy, it can be sorted as electric double layer capacitor (EDLC) and pseudocapacitor. Stoller *et al.* reported a novel graphene-based supercapacitor from chemically modified graphene, showing excellent performance with specific capacitances of 135 and 99 F g^{-1} in aqueous and organic electrolytes, respectively.[104] Nanostructured metal oxide–graphene hybrids such as SnO_2, ZnO, MnO_2/graphene, were widely used for supercapacitor applications.[106–108] Supercapacitor devices based on CCG and polyaniline (PANI) nanofibers films and composites displayed high capacitance of 210 F g^{-1} at 0.3 A g^{-1} and 480 F g^{-1} at 0.1 A g^{-1}, respectively.[109,110] Wang *et al.* reported that single-crystalline $Ni(OH)_2$ hexagonal nanoplates directly grown on GNS could exhibit a high specific capacitance of 1335 F g^{-1} at a charge and discharge current density of 2.8 A g^{-1} and 953 F g^{-1} at 45.7 A g^{-1} with excellent cycling ability.[27]

Recently, noncovalent functionalization of graphene with 1-pyrenecarboxylic acid was employed to fabricate multifunctional devices such as highly sensitive and selective sensors (resistance changes >10 000% in saturated ethanol vapor), and supercapacitors with extremely high specific capacitance (120 F g^{-1}), power density (105 kW kg^{-1}), and energy density (9.2 Wh kg^{-1}).[111]

In addition, functionalized graphene films have also emerged as an interesting alternative electrode material in solar cells.[112–114]

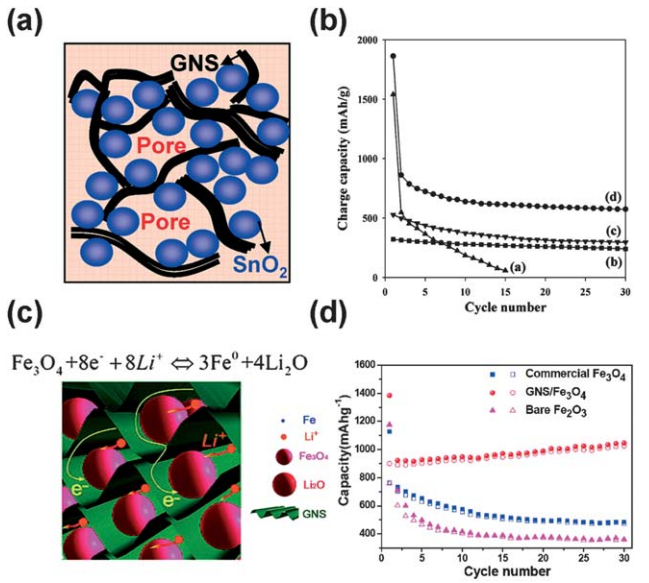

Fig. 11 (a) Schematic of the structure of SnO_2/GNS (b) Cyclic performances for (a) bare SnO_2 NPs; (b) graphite; (c) GNS; (d) SnO_2/GNS. (c) Schematic of a flexible interleaved structure consisting of GNSs and Fe_3O_4 particles. (d) Cycling performance of the commercial Fe_3O_4 particles, Fe_3O_4/GNS composites and bare Fe_2O_3 particles at a current density of 35 mA g^{-1}. Solid symbols, discharge; hollow symbols, charge. Reproduced with permission from ref. 101 (a, b) and ref. 103 (c, d). Copyright: 2009 (a, b) and 2010 (c, d) American Chemical Society.

4. Conclusions and outlook

Liquid-phase exfoliation process opens up a promising approach to scale up the production of graphene. Although GO exfoliation gives the highest concentration in organic solvent or water dispersions, it faces some significant demerits. Due to the irreversible induced destruction in the π-orbital conjugated structures by oxidation, the degradation of the electronic properties, which make graphene unique, can hardly be completely recovered by a chemical reduction process. Specific evidence of poor electronic properties can be found by the low conductivity in cast films and low on–off ratio in its FETs. Solution processing of high-quality graphene exfoliated directly from pure graphite in NMP simply overcomes these weak points, retaining its high electrical performance with few structural defects. However, this process is not perfect. Some solvents, such as NMP, are expensive and toxic with a high-boiling point, requiring special treatment when handling. Meanwhile, many applications are ruled out by the need of using high-boiling-point and toxic solvents. The subsequent aqueous exfoliation generally makes the production "greener" and possible in low-cost manner. Meanwhile, a charged surface of graphene with adsorbed surfactants avoids rapid aggregation. Furthermore, graphene dispersed in an aqueous environment greatly facilitates post-processing such as deposition on a variety of substrates or filtration to form a thin film on membranes.

Of all the methods discussed above, self-exfoliation without sonication seems to be more promising due to its low-energy input, high-quality and high-concentration output. Obviously, the resulting graphene size is directly restricted to the starting graphite size which is typically around several millimetres. Future challenges should aim to address the problems with uncontrollable and random size and layer number in liquid-phase exfoliation, which still limits the applications of graphene. At the same time, aggregation of graphene must be avoided and a high concentration of monolayers of graphene or GNRs must be achieved.

With all the merits from liquid-phase exfoliated graphene, it is efficient to modulate its properties by functionalization through wet chemical routes. Experimental studies of functionalization demonstrate that not only the electronic properties but also the chemical properties of graphene can be modulated, and make it unique in all kinds of applications. However, to the best of our

knowledge, relatively less theoretical work was conducted on understanding the modified parts with graphene. It is highly suggested that the future work should emphasize the understanding of functional parts in the system and then design the desired materials. With precise control of the properties of graphene, it is expected that more interesting applications will be developed with predicted functionalities.

Acknowledgements

This work was partially supported by the National Nature Science of Foundation of China (NSFC) (21051002, 20941003), the National Basic Research Program of China (2010CB934601), the Doctoral Program (20090001120010) and New Century Talent (NCET-09-0177) of the Education Ministry of China, Yok Ying Tung Found (122043), Beijing Outstanding Talent Program (2009D013001000013) and New Star Program of BCST (2008B02). The author would like to express sincere gratitude to present group members who contributed to the preparation of this manuscript, as well as to the former group member, Dr Wen Qian, for her assistance on the research of graphene. We also thank Mr Michael Vosgueritchian at Stanford University for his kind help on revising the manuscript.

Notes and references

1 K. S. Novoselov, A. K. Geim, S. V. Morozov, D. Jiang, Y. Zhang, S. V. Dubonos, I. V. Grigorieva and A. A. Firsov, *Science*, 2004, **306**, 666–669.
2 A. K. Geim and K. S. Novoselov, *Nat. Mater.*, 2007, **6**, 183–191.
3 H. W. Kroto, J. R. Heath, S. C. Obrien, R. F. Curl and R. E. Smalley, *Nature*, 1985, **318**, 162–163.
4 S. Iijima, *Nature*, 1991, **354**, 56–58.
5 K. I. Bolotin, K. J. Sikes, Z. Jiang, M. Klima, G. Fudenberg, J. Hone, P. Kim and H. L. Stormer, *Solid State Commun.*, 2008, **146**, 351–355.
6 A. A. Balandin, S. Ghosh, W. Z. Bao, I. Calizo, D. Teweldebrhan, F. Miao and C. N. Lau, *Nano Lett.*, 2008, **8**, 902–907.
7 C. Lee, X. Wei, J. W. Kysar and J. Hone, *Science*, 2008, **321**, 385–388.
8 J. van den Brink, *Nat. Nanotechnol.*, 2007, **2**, 199–201.
9 C. N. R. Rao, K. Biswas, K. S. Subrahmanyam and A. Govindaraj, *J. Mater. Chem.*, 2009, **19**, 2457–2469.
10 R. R. Nair, P. Blake, A. N. Grigorenko, K. S. Novoselov, T. J. Booth, T. Stauber, N. M. R. Peres and A. K. Geim, *Science*, 2008, **320**, 1308.
11 S. Bae, H. Kim, Y. Lee, X. F. Xu, J. S. Park, Y. Zheng, J. Balakrishnan, T. Lei, H. R. Kim, Y. I. Song, Y. J. Kim, K. S. Kim, B. Ozyilmaz, J. H. Ahn, B. H. Hong and S. Iijima, *Nat. Nanotechnol.*, 2010, **5**, 574–578.
12 X. Li, Y. Zhu, W. Cai, M. Borysiak, B. Han, D. Chen, R. D. Piner, L. Colombo and R. S. Ruoff, *Nano Lett.*, 2009, **9**, 4359–4363.
13 K. S. Kim, Y. Zhao, H. Jang, S. Y. Lee, J. M. Kim, K. S. Kim, J.-H. Ahn, P. Kim, J.-Y. Choi and B. H. Hong, *Nature*, 2009, **457**, 706–710.
14 B. Lang, *Surf. Sci.*, 1975, **53**, 317–329.
15 Y. B. Zhang, J. P. Small, M. E. S. Amori and P. Kim, *Phys. Rev. Lett.*, 2005, **94**, 176803.
16 M. Lotya, P. J. King, U. Khan, S. De and J. N. Coleman, *ACS Nano*, 2010, **4**, 3155–3162.
17 J. N. Coleman, *Adv. Funct. Mater.*, 2009, **19**, 3680–3695.
18 Y. Hernandez, V. Nicolosi, M. Lotya, F. M. Blighe, Z. Sun, S. De, I. T. McGovern, B. Holland, M. Byrne, Y. K. Gun'Ko, J. J. Boland, P. Niraj, G. Duesberg, S. Krishnamurthy, R. Goodhue, J. Hutchison, V. Scardaci, A. C. Ferrari and J. N. Coleman, *Nat. Nanotechnol.*, 2008, **3**, 563–568.
19 J. Robinson, X. J. Weng, K. Trumbull, R. Cavalero, M. Wetherington, E. Frantz, M. LaBella, Z. Hughes, M. Fanton and D. Snyder, *ACS Nano*, 2010, **4**, 153–158.
20 N. Camara, G. Rius, J. R. Huntzinger, A. Tiberj, L. Magaud, N. Mestres, P. Godignon and J. Camassel, *Appl. Phys. Lett.*, 2008, **93**, 263102.
21 X. B. Wang, H. J. You, F. M. Liu, M. J. Li, L. Wan, S. Q. Li, Q. Li, Y. Xu, R. Tian, Z. Y. Yu, D. Xiang and J. Cheng, *Chem. Vap. Deposition*, 2009, **15**, 53–56.
22 X. S. Li, W. W. Cai, J. H. An, S. Kim, J. Nah, D. X. Yang, R. Piner, A. Velamakanni, I. Jung, E. Tutuc, S. K. Banerjee, L. Colombo and R. S. Ruoff, *Science*, 2009, **324**, 1312–1314.
23 A. Peigney, C. Laurent, E. Flahaut, R. R. Bacsa and A. Rousset, *Carbon*, 2001, **39**, 507–514.
24 X. Wang, X. Li, L. Zhang, Y. Yoon, P. K. Weber, H. Wang, J. Guo and H. Dai, *Science*, 2009, **324**, 768–771.
25 V. C. Tung, M. J. Allen, Y. Yang and R. B. Kaner, *Nat. Nanotechnol.*, 2008, **4**, 25–29.
26 D. Wei, Y. Liu, Y. Wang, H. Zhang, L. Huang and G. Yu, *Nano Lett.*, 2009, **9**, 1752–1758.
27 H. L. Wang, H. S. Casalongue, Y. Y. Liang and H. J. Dai, *J. Am. Chem. Soc.*, 2010, **132**, 7472–7477.
28 G. M. Scheuermann, L. Rumi, P. Steurer, W. Bannwarth and R. Mülhaupt, *J. Am. Chem. Soc.*, 2009, **131**, 8262–8270.
29 D. Wang, D. Choi, J. Li, Z. Yang, Z. Nie, R. Kou, D. Hu, C. Wang, L. V. Saraf, J. Zhang, I. A. Aksay and J. Liu, *ACS Nano*, 2009, **3**, 907–914.
30 D. R. Dreyer, S. Park, C. W. Bielawski and R. S. Ruoff, *Chem. Soc. Rev.*, 2010, **39**, 228–240.
31 C. Soldano, A. Mahmood and E. Dujardin, *Carbon*, 2010, **48**, 2127–2150.
32 M. J. Allen, V. C. Tung and R. B. Kaner, *Chem. Rev.*, 2010, **110**, 132–145.
33 W. Choi, I. Lahiri, R. Seelaboyina and Y. S. Kang, *Crit. Rev. Solid State Mat. Sci.*, 2010, **35**, 52–71.
34 C. N. R. Rao, A. K. Sood, R. Voggu and K. S. Subrahmanyam, *J. Phys. Chem. Lett.*, 2010, **1**, 572–580.
35 D. Chen, L. H. Tang and J. H. Li, *Chem. Soc. Rev.*, 2010, **39**, 3157–3180.
36 D. R. Dreyer, R. S. Ruoff and C. W. Bielawski, *Angew. Chem., Int. Ed.*, 2010, **49**, 9336–9344.
37 W. S. Hummers and R. E. Offeman, *J. Am. Chem. Soc.*, 1958, **80**, 1339.
38 S. Stankovich, D. A. Dikin, R. D. Piner, K. A. Kohlhaas, A. Kleinhammes, Y. Jia, Y. Wu, S. T. Nguyen and R. S. Ruoff, *Carbon*, 2007, **45**, 1558–1565.
39 G. Williams, B. Seger and P. V. Kamat, *ACS Nano*, 2008, **2**, 1487–1491.
40 S. Park, J. H. An, R. D. Piner, I. Jung, D. X. Yang, A. Velamakanni, S. T. Nguyen and R. S. Ruoff, *Chem. Mater.*, 2008, **20**, 6592–6594.
41 G. Wang, J. Yang, J. Park, X. Gou, B. Wang, H. Liu and J. Yao, *J. Phys. Chem. C*, 2008, **112**, 8192–8195.
42 H.-J. Shin, K. K. Kim, A. Benayad, S.-M. Yoon, H. K. Park, I.-S. Jung, M. H. Jin, H.-K. Jeong, J. M. Kim, J.-Y. Choi and Y. H. Lee, *Adv. Funct. Mater.*, 2009, **19**, 1987–1992.
43 H. Wang, J. T. Robinson, X. Li and H. Dai, *J. Am. Chem. Soc.*, 2009, **131**, 9910–9911.
44 S. Dubin, S. Gilje, K. Wang, V. C. Tung, K. Cha, A. S. Hall, J. Farrar, R. Varshneya, Y. Yang and R. B. Kaner, *ACS Nano*, 2010, **4**, 3845–3852.
45 Z.-J. Fan, W. Kai, J. Yan, T. Wei, L.-J. Zhi, J. Feng, Y.-M. Ren, L.-P. Song and F. Wei, *ACS Nano*, 2011, **5**, 191–198.
46 L. X. Benedict, N. G. Chopra, M. L. Cohen, A. Zettl, S. G. Louie and V. H. Crespi, *Chem. Phys. Lett.*, 1998, **286**, 490–496.
47 R. Zacharia, H. Ulbricht and T. Hertel, *Phys. Rev. B: Condens. Matter Mater. Phys.*, 2004, **69**, 155406.
48 M. Lotya, Y. Hernandez, P. J. King, R. J. Smith, V. Nicolosi, L. S. Karlsson, F. M. Blighe, S. De, Z. Wang, I. T. McGovern, G. S. Duesberg and J. N. Coleman, *J. Am. Chem. Soc.*, 2009, **131**, 3611–3620.
49 C.-J. Shih, S. Lin, M. S. Strano and D. Blankschtein, *J. Am. Chem. Soc.*, 2010, **132**, 14638–14648.
50 J. Restolho, J. L. Mata and B. Saramago, *J. Colloid Interface Sci.*, 2009, **340**, 82–86.

51 X. Q. Wang, P. F. Fulvio, G. A. Baker, G. M. Veith, R. R. Unocic, S. M. Mahurin, M. F. Chi and S. Dai, *Chem. Commun.*, 2010, **46**, 4487–4489.
52 W. Qian, R. Hao, Y. Hou, Y. Tian, C. Shen, H. Gao and X. Liang, *Nano Res.*, 2009, **2**, 706–712.
53 B. J. Jiang, C. G. Tian, L. Wang, Y. X. Xu, R. H. Wang, Y. J. Qiao, Y. G. Ma and H. G. Fu, *Chem. Commun.*, 2010, **46**, 4920–4922.
54 I. Janowska, K. Chizari, O. Ersen, S. Zafeiratos, D. Soubane, V. Da Costa, V. Speisser, C. Boeglin, M. Houlle, D. Begin, D. Plee, M. J. Ledoux and C. Pham-Huu, *Nano Res.*, 2010, **3**, 126–137.
55 J. H. Lee, D. W. Shin, V. G. Makotchenko, A. S. Nazarov, V. E. Fedorov, Y. H. Kim, J. Y. Choi, J. M. Kim and J. B. Yoo, *Adv. Mater.*, 2009, **21**, 4383–4387.
56 W. T. Gu, W. Zhang, X. M. Li, H. W. Zhu, J. Q. Wei, Z. Li, Q. K. Shu, C. Wang, K. L. Wang, W. C. Shen, F. Y. Kang and D. H. Wu, *J. Mater. Chem.*, 2009, **19**, 3367–3369.
57 L. M. Viculis, J. J. Mack, O. M. Mayer, H. T. Hahn and R. B. Kaner, *J. Mater. Chem.*, 2005, **15**, 974–978.
58 J. Zheng, C. A. Di, Y. Q. Liu, H. T. Liu, Y. L. Guo, C. Y. Du, T. Wu, G. Yu and D. B. Zhu, *Chem. Commun.*, 2010, **46**, 5728–5730.
59 Z. Z. Sun, S. Kohama, Z. X. Zhang, J. R. Lomeda and J. M. Tour, *Nano Res.*, 2010, **3**, 117–125.
60 R. Hao, W. Qian, L. H. Zhang and Y. L. Hou, *Chem. Commun.*, 2008, 6576–6578.
61 X. Li, X. Wang, L. Zhang, S. Lee and H. Dai, *Science*, 2008, **319**, 1229–1232.
62 D. V. Kosynkin, A. L. Higginbotham, A. Sinitskii, J. R. Lomeda, A. Dimiev, B. K. Price and J. M. Tour, *Nature*, 2009, **458**, 872–876.
63 L. Jiao, L. Zhang, X. Wang, G. Diankov and H. Dai, *Nature*, 2009, **458**, 877–880.
64 M. Han, B. Özyilmaz, Y. Zhang and P. Kim, *Phys. Rev. Lett.*, 2007, **98**, 206805.
65 X. Wang, Y. Ouyang, X. Li, H. Wang, J. Guo and H. Dai, *Phys. Rev. Lett.*, 2008, **100**, 206803.
66 L. Tapasztó, G. Dobrik, P. Lambin and L. P. Biró, *Nat. Nanotechnol.*, 2008, **3**, 397–401.
67 S. S. Datta, D. R. Strachan, S. M. Khamis and A. T. C. Johnson, *Nano Lett.*, 2008, **8**, 1912–1915.
68 L. Ci, Z. Xu, L. Wang, W. Gao, F. Ding, K. F. Kelly, B. I. Yakobson and P. M. Ajayan, *Nano Res.*, 2008, **1**, 116–122.
69 J. Campos-Delgado, J. M. Romo-Herrera, X. T. Jia, D. A. Cullen, H. Muramatsu, Y. A. Kim, T. Hayashi, Z. F. Ren, D. J. Smith, Y. Okuno, T. Ohba, H. Kanoh, K. Kaneko, M. Endo, H. Terrones, M. S. Dresselhaus and M. Terrones, *Nano Lett.*, 2008, **8**, 2773–2778.
70 J. Lu, J.-X. Yang, J. Wang, A. Lim, S. Wang and K. P. Loh, *ACS Nano*, 2009, **3**, 2367–2375.
71 N. W. Pu, C. A. Wang, Y. Sung, Y. M. Liu and M. D. Ger, *Mater. Lett.*, 2009, **63**, 1987–1989.
72 N. Liu, F. Luo, H. X. Wu, Y. H. Liu, C. Zhang and J. Chen, *Adv. Funct. Mater.*, 2008, **18**, 1518–1525.
73 C. Vallés, C. Drummond, H. Saadaoui, C. A. Furtado, M. He, O. Roubeau, L. Ortolani, M. Monthioux and A. Pénicaud, *J. Am. Chem. Soc.*, 2008, **130**, 15802–15804.
74 N. Behabtu, J. R. Lomeda, M. J. Green, A. L. Higginbotham, A. Sinitskii, D. V. Kosynkin, D. Tsentalovich, A. N. G. Parra-Vasquez, J. Schmidt, E. Kesselman, Y. Cohen, Y. Talmon, J. M. Tour and M. Pasquali, *Nat. Nanotechnol.*, 2010, **5**, 406–411.
75 G. Van Lier, C. Van Alsenoy, V. Van Doren and P. Geerlings, *Chem. Phys. Lett.*, 2000, **326**, 181–185.
76 C. D. Reddy, S. Rajendran and K. M. Liew, *Nanotechnology*, 2006, **17**, 864–870.
77 K. N. Kudin, G. E. Scuseria and B. I. Yakobson, *Phys. Rev. B*, 2001, **64**, 235406.
78 C. Gomez-Navarro, M. Burghard and K. Kern, *Nano Lett.*, 2008, **8**, 2045–2049.
79 D. A. Dikin, S. Stankovich, E. J. Zimney, R. D. Piner, G. H. B. Dommett, G. Evmenenko, S. T. Nguyen and R. S. Ruoff, *Nature*, 2007, **448**, 457–460.
80 S. Park, K.-S. Lee, G. Bozoklu, W. Cai, S. T. Nguyen and R. S. Ruoff, *ACS Nano*, 2008, **2**, 572–578.
81 S. Park, D. A. Dikin, S. T. Nguyen and R. S. Ruoff, *J. Phys. Chem. C*, 2009, **113**, 15801–15804.
82 S. Y. Zhou, G. H. Gweon, A. V. Fedorov, P. N. First, W. A. De Heer, D. H. Lee, F. Guinea, A. H. C. Neto and A. Lanzara, *Nat. Mater.*, 2007, **6**, 770–775.
83 N. Li, Z. Y. Wang, K. K. Zhao, Z. J. Shi, Z. N. Gu and S. K. Xu, *Carbon*, 2010, **48**, 255–259.
84 X. L. Li, H. L. Wang, J. T. Robinson, H. Sanchez, G. Diankov and H. J. Dai, *J. Am. Chem. Soc.*, 2009, **131**, 15939–15944.
85 K. Carva, B. Sanyal, J. Fransson and O. Eriksson, *Phys. Rev. B: Condens. Matter Mater. Phys.*, 2010, **81**, 245405.
86 A. Sinitskii, A. Dimiev, D. A. Corley, A. A. Fursina, D. V. Kosynkin and J. M. Tour, *ACS Nano*, 2010, **4**, 1949–1954.
87 G. Lu, S. Park, K. Yu, R. S. Ruoff, L. E. Ocola, D. Rosenmann and J. Chen, *ACS Nano*, 2011, **5**, 1154–1164.
88 J. Lu, I. Do, L. T. Drzal, R. M. Worden and I. Lee, *ACS Nano*, 2008, **2**, 1825–1832.
89 Y. X. Fang, S. J. Guo, C. Z. Zhu, Y. M. Zhai and E. K. Wang, *Langmuir*, 2010, **26**, 11277–11282.
90 C. S. Shan, H. F. Yang, D. X. Han, Q. X. Zhang, A. Ivaska and L. Niu, *Biosens. Bioelectron.*, 2010, **25**, 1504–1508.
91 Z. Wang, X. Zhou, J. Zhang, F. Boey and H. Zhang, *J. Phys. Chem. C*, 2009, **113**, 14071–14075.
92 C. Xu, X. Wang and J. Zhu, *J. Phys. Chem. C*, 2008, **112**, 19841–19845.
93 F. H. Li, H. F. Yang, C. S. Shan, Q. X. Zhang, D. X. Han, A. Ivaska and L. Niu, *J. Mater. Chem.*, 2009, **19**, 4022–4025.
94 L. F. Dong, R. R. S. Gari, Z. Li, M. M. Craig and S. F. Hou, *Carbon*, 2010, **48**, 781–787.
95 Y. M. Li, L. H. Tang and J. H. Li, *Electrochem. Commun.*, 2009, **11**, 846–849.
96 H. Y. Li, X. H. Zhang, H. L. Pang, C. T. Huang and J. H. Chen, *J. Solid State Electrochem.*, 2010, **14**, 2267–2274.
97 Y. Li, X. Fan, J. Qi, J. Ji, S. Wang, G. Zhang and F. Zhang, *Mater. Res. Bull.*, 2010, **45**, 1413–1418.
98 Y. Wang, Y. Y. Shao, D. W. Matson, J. H. Li and Y. H. Lin, *ACS Nano*, 2010, **4**, 1790–1798.
99 H. Liu, J. Gao, M. Q. Xue, N. Zhu, M. N. Zhang and T. B. Cao, *Langmuir*, 2009, **25**, 12006–12010.
100 E. Yoo, J. Kim, E. Hosono, H. Zhou, T. Kudo and I. Honma, *Nano Lett.*, 2008, **8**, 2277–2282.
101 S. M. Paek, E. Yoo and I. Honma, *Nano Lett.*, 2009, **9**, 72–75.
102 Z. S. Wu, W. C. Ren, L. Wen, L. B. Gao, J. P. Zhao, Z. P. Chen, G. M. Zhou, F. Li and H. M. Cheng, *ACS Nano*, 2010, **4**, 3187–3194.
103 G. M. Zhou, D. W. Wang, F. Li, L. L. Zhang, N. Li, Z. S. Wu, L. Wen, G. Q. Lu and H. M. Cheng, *Chem. Mater.*, 2010, **22**, 5306–5313.
104 M. D. Stoller, S. Park, Y. Zhu, J. An and R. S. Ruoff, *Nano Lett.*, 2008, **8**, 3498–3502.
105 D. Pan, S. Wang, B. Zhao, M. Wu, H. Zhang, Y. Wang and Z. Jiao, *Chem. Mater.*, 2009, **21**, 3136–3142.
106 F. H. Li, J. F. Song, H. F. Yang, S. Y. Gan, Q. X. Zhang, D. X. Han, A. Ivaska and L. Niu, *Nanotechnology*, 2009, **20**, 455602.
107 Y. Zhang, H. Li, L. Pan, T. Lu and Z. Sun, *J. Electroanal. Chem.*, 2009, **634**, 68–71.
108 S. Chen, J. Zhu, X. Wu, Q. Han and X. Wang, *ACS Nano*, 2010, **4**, 2822–2830.
109 Q. Wu, Y. X. Xu, Z. Y. Yao, A. R. Liu and G. Q. Shi, *ACS Nano*, 2010, **4**, 1963–1970.
110 K. Zhang, L. L. Zhang, X. S. Zhao and J. Wu, *Chem. Mater.*, 2010, **22**, 1392–1401.
111 X. An, T. Simmons, R. Shah, C. Wolfe, K. M. Lewis, M. Washington, S. K. Nayak, S. Talapatra and S. Kar, *Nano Lett.*, 2010, **10**, 4295–4301.
112 Z. F. Liu, Q. Liu, Y. Huang, Y. F. Ma, S. G. Yin, X. Y. Zhang, W. Sun and Y. S. Chen, *Adv. Mater.*, 2008, **20**, 3924–3930.
113 W. Hong, Y. Xu, G. Lu, C. Li and G. Shi, *Electrochem. Commun.*, 2008, **10**, 1555–1558.
114 L. Valentini, M. Cardinali, S. B. Bon, D. Bagnis, R. Verdejo, M. A. Lopez-Manchado and J. M. Kenny, *J. Mater. Chem.*, 2010, **20**, 995–1000.

